International Journal of Mass Spectrometry 299 (2011) 27–34

Contents lists available at ScienceDirect

International Journal of Mass Spectrometry

journal homepage: www.elsevier.com/locate/ijms

Precise thermal ionization mass spectrometric measurements of $^{142}Nd/^{144}Nd$ and $^{143}Nd/^{144}Nd$ isotopic ratios of Nd separated from geological standards by chromatographic methods

A. Ali, G. Srinivasan*

Cosmochemistry Laboratory, Department of Geology, University of Toronto, 22 Russell Street, Toronto, ON, M5S 3B1, Canada

ARTICLE INFO

Article history:
Received 3 May 2010
Received in revised form
13 September 2010
Accepted 13 September 2010
Available online 17 September 2010

Keywords:
Ion exchange chromatography
Neodymium
Isotope
TIMS

ABSTRACT

A chromatographic separation technique for $^{142}Nd/^{144}Nd$ and $^{143}Nd/^{144}Nd$ isotope ratio measurements is established and applied to the analyses of geological standards of basaltic compositions (BCR-2, BIR-1) using Isoprobe-T TIMS. The instrument was tested for reliability and reproducibility to measure Nd isotope composition using the synthetic standard JNdi-1. The techniques were also applied to a carbonatite lava sample, OL-6, Oldoinyo Lengai, to check the validity of method for carbonatite matrix. The isotope ratios of $^{143}Nd/^{144}Nd$ for synthetic Nd standard JNdi-1, geological standards BCR-2, BIR-1, and carbonatite lava sample OL-6 obtained by these methods are in good agreement with previously published data. The $^{143}Nd/^{144}Nd$ values for JNdi-1 and BCR-2 have an external precision of ±13 ppm and ±15 ppm (2σ), respectively. The JNdi-1 and BCR-2 data for $^{142}Nd/^{144}Nd$ has an external precision of ±12 ppm and ±8 ppm (2σ), respectively. The $^{142}Nd/^{144}Nd$ composition of the two geological standards BCR-2 and BIR-1 are indistinguishable from synthetic mono-element standard JNdi-1, and they all fall within the 12 ppm (2σ) envelope of external precision. The external reproducibility is sufficient to distinguish and resolve 20 ppm anomalies in $^{142}Nd/^{144}Nd$ values.

1. Introduction

The decay products of radiogenic isotopes have proved to be powerful tools to understand the chemical evolution of planetary bodies. The Sm–Nd radiogenic decay system includes the coupled ^{147}Sm–^{143}Nd and ^{146}Sm–^{142}Nd chronometers which are useful for geochemical and cosmochemical studies. Sm–Nd radiogenic system is one of the most robust chronometers utilized to trace the long-term chemical evolution of the silicate portion of the Earth via long-lived radioisotope ^{147}Sm ($T_{1/2}$ (half-life) ~106 Ga) as well as short-lived ^{146}Sm ($T_{1/2}$ ~103 Ma) isotope. Both parent (Sm) and daughter (Nd) are refractory lithophile elements, and are therefore, unaffected either by volatile loss or core formation event in the early history of the Earth. Chondritic meteorites show a 20 ppm deficit in $^{142}Nd/^{144}Nd$ [1] compared to the terrestrial samples which indicates that 70–90% of the Earth's mantle is compositionally similar to the incompatible element-depleted source of MORB, possibly as a result of global differentiation which took place around ~4.53 Ga, within 30 Ma of Earth's creation. The excess of ^{142}Nd in rocks from Isua greenstone belt [2] in west Greenland originated from the mantle source with higher Sm/Nd ratio while the complimentary mantle reservoir, with lower Sm/Nd composition, was recently discovered in the Nuvvuagittuq greenstone belt, Quebec, Canada [3]. Alternatively, the budget of Sm and Nd in the silicate mantle and the isotopic evolution of ^{143}Nd and ^{142}Nd could be affected by later accretion of parts of differentiated planetesimals, a scenario which does not necessitate [4] the existence of hidden reservoirs as postulated previously [1,3]. The low initial abundance of extinct ^{146}Sm in the Solar System, $^{146}Sm/^{144}Sm$ ~0.0085 [5], and the small differences in compatibility of Sm and Nd result in extremely small variations in ^{142}Nd abundances between different planetary reservoirs. Application of ^{146}Sm–^{142}Nd systematics to different planetary reservoirs therefore requires determination of small variations in ^{142}Nd abundance through measurement of $^{142}Nd/^{144}Nd$ ratio with an external precision of ~10 ppm for meaningful resolution of data. In recent studies both MC-ICPMS [6,7] and TIMS [1–5,8–10] techniques have been used for the determination of $^{142}Nd/^{144}Nd$ and $^{143}Nd/^{144}Nd$ ratios in terrestrial samples. For example from the same laboratory, the $^{143}Nd/^{144}Nd$ ratios obtained for BCR-2 geological standards by MC-ICPMS is 0.512637 ± 17 (2σ, $n = 10$) and TIMS 0.512634 ± 12 (2σ, $n = 11$) [7]. These mean values [7] overlap within errors and differ from each other by 5 ppm, and compared to MC-ICPMS, the data obtained by TIMS has a better external precision. In several recent studies using TIMS has produced excellent external precisions on

* Corresponding author. Tel.: +1 416 946 0278; fax: +1 416 978 3938.
E-mail addresses: ali@geology.utoronto.ca (A. Ali), srini@geology.utoronto.ca (G. Srinivasan).

1387-3806/$ – see front matter
doi:10.1016/j.ijms.2010.09.014

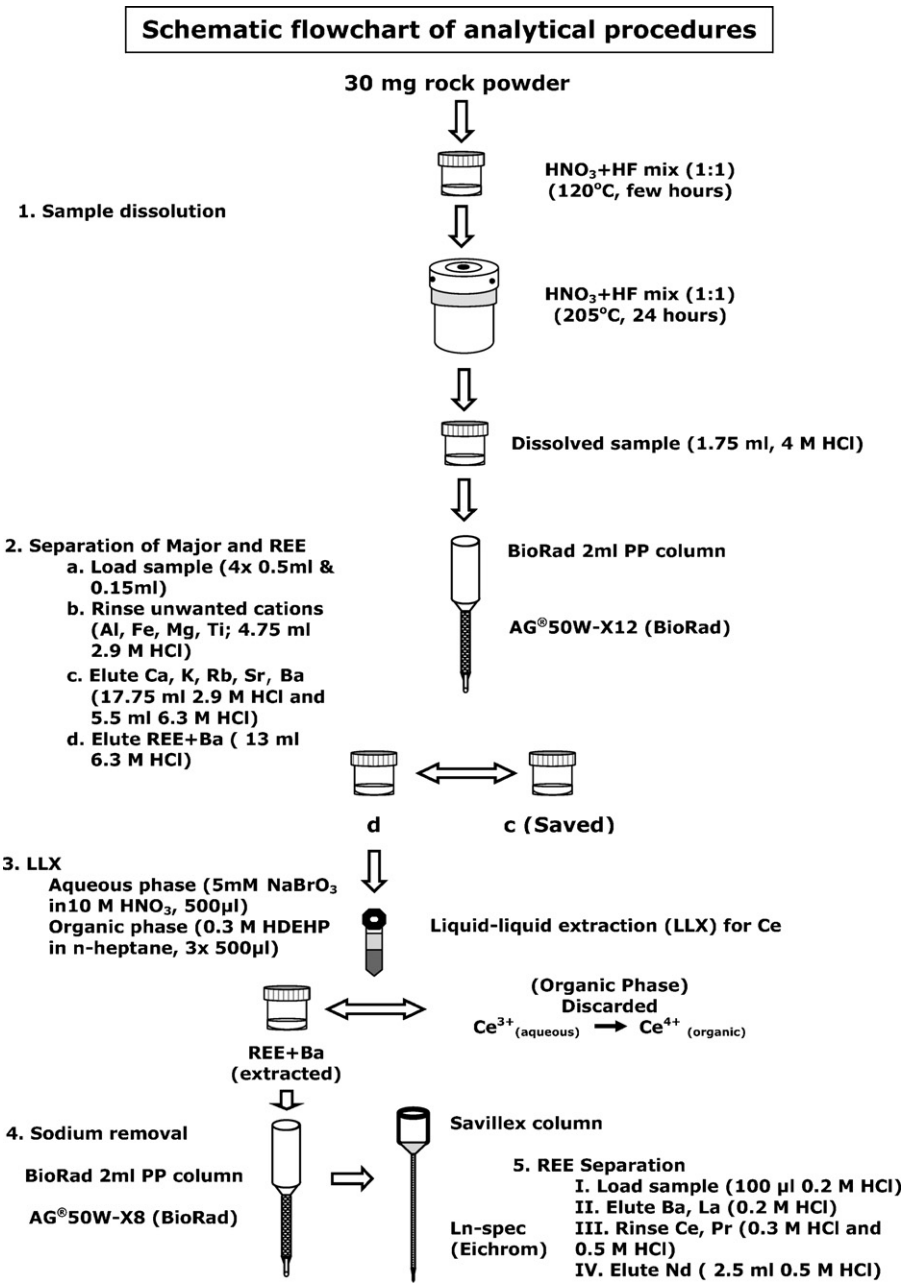

Fig. 1. Sample digestion and processing scheme for separating high purity Nd from rock samples. Item #1 describes method for digesting rock powders for loading on ion exchange columns. Items 2, 3 and 4 describe the steps for isolating REE fraction; removing Ce from the REE fraction; removing excess Na introduced during step 3; and isolating Nd from all other REEs including Sm in step 5.

$^{142}Nd/^{144}Nd$ ratio of AMES standard of 2 ppm (2σ) [2], 3 ppm (2σ) [8], and 3.5 ppm (2σ) [9] by loading 300–500, 600–900 and 600 ng of Nd, respectively. For La Jolla and JNdi-1 [1,11] the external precisions are better than 6 ppm (2σ), however, the Nd load is not reported. For a ~300 ng load of CIT nNd-β [10] reference standard an external precision of 6 ppm was obtained [12].

The isotope ratio determinations by TIMS require high quality chemical separation of Sm and Nd from the rock samples for analyses in mass spectrometer. For example an impure sample of Nd will reduce ion yield and cause beam instability potentially resulting in a poor precision and reproducibility [13]. Furthermore, impurities of Ce and Sm will cause isobaric interference which requires correction further inhibiting the quality of analyses. The results from a three column technique for the separation of high purity Nd from rock reference materials for isotopic analyses using TIMS are reported here. Nd isotope composition of the mono-element standard JNdi-1 [14], and geological standards BCR-2 [15,16], BIR-1 [17,18] and a carbonatite lava sample (OL-6) from Oldoinyo Lengai [19] using the above techniques and measured using the Isoprobe-T TIMS are also reported.

2. Sample preparation

2.1. Reagents and materials

All working solutions and acids were prepared using >18.2 MΩ cm^{-1} H_2O from a Milli-Q water system (Millipore Corporation). Trace metal grade hydrochloric and nitric acids were further purified at sub-boiling temperatures using custom PTFE distillers (Savillex, Minnetonka). Hydrofluoric and perchloric acids

of baseline grade (from Seastar Chemicals Inc.) with certified trace element (e.g., Ce, Nd, Sm) blanks of <1 ppt were used without further purification. The major elements (e.g., Mg, Ca, Fe) were separated from Ba and rare earth element (REE) fraction using AG®50W-X12 (BioRad, 200–400 mesh particle size, hydrogen-form) in 2 ml columns (BioRad). Subsequently Ba, La, Nd, and Sm were separated from the Ba and REE fraction obtained from the first column using Ln-spec resin (HDEHP-based, 50–100 mesh particle size, Eichrom) in commercially available PFA columns (Savillex, Minnetonka, USA). Experiments were performed in class-100 clean air work stations with acid-cleaned apparatus and plastic-ware.

2.2. Sample dissolution

The schematic for rock dissolution is described in Item #1 of Fig. 1. Whole rock powdered samples weighing ~25–30 mg were dissolved in a 1:1 mixture of concentrated HNO_3 and HF using 15 ml PFA vials (Savillex Corporation, USA). The samples were heated for few hours at 120 °C and then completely dried at the same temperature to remove silicon. The dried samples were treated by 1:1 mixture of concentrated HNO_3 and HF using Teflon bomb (Parr Instrument Co.) in the oven at 205 °C for 24 h to ensure complete digestion of any residue. The digested samples were routinely examined under the microscope and centrifuged to confirm complete digestion. The fluorides (CaF_2, MgF_2) were removed by evaporating with a 1:2 mixture of concentrated $HClO_4$ and 6 M HCl at controlled heating. The samples were converted into chloride salts by drying two times with 0.5 ml of 6 M HCl.

Other studies have adopted only Savillex vial without using Teflon bomb for digestion. For example, the potential risk of incomplete dissolution of zircons in felsic metasediments and orthogneisses from Isua Greenstone belt is not taken into consideration because in situ decay of ^{146}Sm in zircon would only increase the $^{142}Nd/^{144}Nd$ ratio in a 3.8 Ga old rock by only 0.1 ppm [2]. Therefore it is extremely unlikely to have biased the measured ^{142}Nd signatures as 0.1 ppm is well below the resolution capability of any measurement technique available so far. A two stage dissolution technique was adopted for this study, i.e., Savillax vial for breaking down the silicates and removing the silicon and a Teflon bomb digestion to dissolve any undigested refractory residue. These procedures were optimized for dissolving whole-rock powders to study Nd isotope composition are applicable for any sample containing refractory phases which can potentially influence the contribution to ^{142}Nd signature.

2.3. Cation-exchange separation (first column)

The digested samples were dissolved in 4 M HCl and loaded onto the first column. The separation of alkalis (K, Ca, Rb, Sr) and REE (La, Nd, Sm) was achieved using 2 ml capacity BioRad column filled with AG®50W-X12 resin, pre-cleaned with 6 M HCl and pre-conditioned with 4 M HCl (Fig. 1). After loading sample onto the resin, Al, Fe and Mg were washed out by eluting 4.75 ml of 2.9 M HCl (Table 1, Fig. 1). The fraction of other cations such as K, Ca, Rb and Sr were collected by eluting 17.75 ml of 2.9 M HCl and followed by 5.5 ml of 6.3 M HCl. The LREE fraction containing Sm and Nd with a substantial cut of Ce (~40%), Ba and other REEs were extracted from the resin by eluting 13 ml of 6.3 M HCl. To elute complete REE fraction including Ba ~26 ml is required.

2.4. Separation of pure Nd

A significant proportion of Ce was cut (~40%) in the LREE fraction from the first column, the remaining quantity of Ce in the LREE fraction (13 ml) obtained from the first column was further removed by liquid–liquid extraction [20]. Precise measurements of $^{142}Nd/^{144}Nd$ ratios require efficient Ce removal from Nd such that $^{142}Ce/^{142}Nd$ ratio of ~1 in crustal rocks (Ce/Nd = 1.34 for silicate Earth) [21] is reduced to about 10^{-6} [2]. A synthetic mixture of Ce and Nd in the same proportion and with abundance equivalent to that of ~30 mg of BCR-2 was analyzed using TIMS to measure ($^{140}Ce^+/^{142}Nd^+$) and estimate ($^{142}Ce^+/^{142}Nd^+$) as a proxy measure for separation of Ce from Nd. The liquid–liquid separation is very efficient in separating Ce from Nd and the estimated ($^{142}Ce^+/^{142}Nd^+$) is 13×10^{-6} which is insufficient for our purpose. The combination of liquid–liquid extraction along with elution through Ln-spec resin results estimated ratio of ($^{142}Ce^+/^{142}Nd^+$) of $<3 \times 10^{-6}$ that is satisfactory for ^{142}Nd measurement. The added advantage of elution through Ln-spec resin is removal of all REEs including Sm which is a major interfering species.

For the liquid–liquid extraction (Table 1 and Fig. 1) the aqueous phase is prepared by mixing 5 millimolar (mM) sodium bromate ($NaBrO_3$, Alfa Aesar) solution in 10 M HNO_3 and the organic phases are 3 M HDEHP (di-2-ethylhexyl phosphoric acid, Alfa Aesar) and pure n-heptane (HPLC Grade, Fisher Scientific). The oxidation of Ce^{3+} in the aqueous phase to Ce^{4+} isolates Ce from the rest of REE^{3+} to form an organic complex with HDEHP. This step is repeated thrice for complete oxidation of Ce. Traces of dissolved HDEHP in the aqueous phase containing the remaining REE^{3+} were removed by scrubbing with n-heptane (Table 1 and Fig. 1). The bromate in aqueous phase (containing REE^{3+}) was destroyed by drying in 0.1 ml of 6 M HCl several times. The abundant Na was removed from the REE^{3+} fraction using a second column (2 ml BioRad) filled with cation-exchange resin, AG®50W-X8 (200–400 mesh particle size, hydrogen-form, BioRad).

After Ce extraction and Na removal the LREE fraction was dissolved in 100 μl of 0.2 M HCl and loaded onto the third column (4 mm internal diameter × 20 cm height) filled with Ln-resin (Eichrom). The outline of the technique for separating Nd is shown in Table 1 and Fig. 1 This technique is typically repeated twice on

Table 1
Outline of the Nd purification procedures, LLX and HDEHP stand for liquid–liquid extraction and di-(2-ethylhexyl) phosphoric acid, respectively.

Steps	Details	Volume
First column (2 ml capacity, BioRad)		
Resin	AG®50W-X12 (200–400 mesh, H-form, BioRad)	
Clean	6 M HCl, MQ	10 ml, 5 ml
Condition	4 M HCl	2 ml
Load sample	4 M HCl	1.75 ml
Rinse/elute	2.9 M HCl	22.5 ml
major/minor cations		
	6.3 M HCl	5.5 ml
Elute REE+Ba	6.3 M HCl	13 ml
Liquid–liquid extraction		
REE + Ba fraction	10 M HNO_3	100 μl
Aqueous phase	5 mM $NaBrO_3$ in 10 M HNO_3	500 μl
Organic phase	0.3 M HDEHP in n-heptane	3× 500 μl
Scrub	n-Heptane	3× 500 μl
Second column (2 ml capacity, BioRad)		
Resin	AG®50W-X8 (200–400 mesh, H-form, BioRad)	
Clean	6 M HCl, MQ	10 ml, 5 ml
Condition	2 M HCl	2 ml
Load sample	2 M HCl	200 μl
Rinse Na	2 M HCl	8 ml
Elute REE + Ba by	6 M HCl	10 ml
Third column (2.5 ml capacity, Savillex)		
Resin	Ln-spec (50–100 mesh, HDEHP-based, Eichrom)	
Clean	6 M HCl, MQ	10 ml, 5 ml
Condition	0.2 M HCl	5 ml
Load sample	0.2 M HCl	100 μl
Rinse Ba, La	0.2 M HCl	11.9 ml
Rinse Ce, Pr	0.3 M HCl, 0.5 M HCl	3 ml, 0.75 ml
Elute Nd	0.5 M HCl	2.5 ml
Rinse	0.5 M HCl	3.75 ml
Elute Sm	0.5 M HCl	0.5 ml

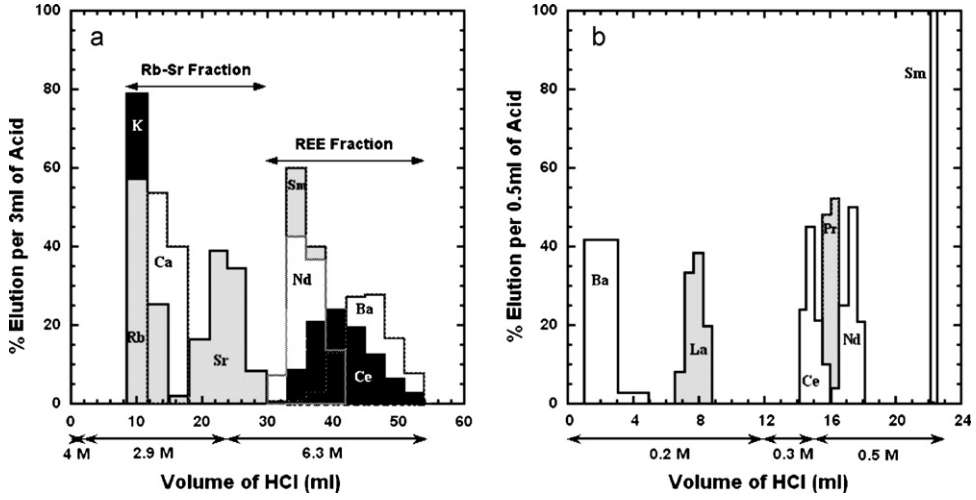

Fig. 2. Panel (a) shows the separation scheme of major and minor cations (e.g., K, Ca, Rb and Sr) and Al, Ti, Fe, Mg (not shown here) and REE + Ba fraction achieved using 2 ml capacity BioRad column (0.8 cm i.d. × 4 cm height) filled with AG®50W-X12 (200–400 mesh size). The column was eluted with hydrochloric acid of varying strength (4 M, 2.9 M and 6.3 M) as noted on the axis. After removing Ce in the REE fraction using liquid–liquid extraction (see text) the remaining REE fraction was eluted using Savillex column (0.4 cm i.d. × 20 cm height) filled with Ln-spec resin (50–100 μm) as shown in panel (b). Elution of REE fraction using weak HCl (0.2–0.5 M) produced the Ba, La, Nd and Sm fractions. The calibration of both columns for elution curves was done with BCR-2 aliquot.

natural rock samples to achieve desired results. The present analytical technique was developed for precise measurement of Nd isotopes; however, using REE fraction (26 ml), separation of La, Ba and Sm can also be achieved with great success (Fig. 2).

3. Mass spectrometry – measurement of Nd isotope ratios

The Nd isotopic ratios were measured using Isoprobe-T TIMS. Nd was measured as metal using zone-refined (HCross) and outgassed Re filaments in a triple filament configuration. Nd (~200–500 ng) was dissolved in 2 microlitre (μl) of 1.5 M HCl and loaded on Re outer filament. The Nd load was preceded and followed by loading 1 μl of 0.1 M high purity phosphoric acid (J.T. Baker Ultrapure Reagent ULTREX LOT#Y09584). The phosphoric acid was gently heated at 0.7 A and evaporated to dryness. The sample of Nd was heated at about 1.2 A and evaporated to dryness. After drying the second load of phosphoric acid the filament was heated to dull red at ~2 A for a few seconds.

Nearly ~500 ng of Nd for JNdi-1 and ~200 ng of Nd from BCR-2 and BIR-1 samples are loaded on Re filament as a chloride. The ionization (center) filament is maintained at a temperature of ~2000 °C by heating it to 4.75 A at a rate of 0.05 A/min. Subsequently the evaporation filament was gently heated at 0.002 A/min to ~2 A till a ^{142}Nd signal of 0.1–1.0 pA (10–100 mV) is obtained. For JNdi-1 samples the ^{142}Nd ion beam signal is optimized to strength of ~50 pA (~5 V) by heating the evaporation (side) filament to ~2.5 A and adjusting the focussing parameters; and centering the magnet. The 7 isotopes of Nd were measured in dynamic mode as 4 sequences (Table 2) to minimize measurement uncertainties due to variations in relative detector efficiencies over the measurement time of 4–8 h for 200–400 ratios, respectively. Typical ^{142}Nd signal strength for

Table 2
Dynamic 4 sequence matrix for Nd isotope ratio measurement.

Sequence	L2	Ax	H1	H2	H3	H4	H5	H6
S1	^{139}La$^+$	^{141}Pr$^+$	^{142}Nd$^+$	^{143}Nd$^+$	^{144}Nd$^+$	^{145}Nd$^+$	^{146}Nd$^+$	^{147}Sm$^+$
Interference			^{142}Ce$^+$		^{144}Sm$^+$			
S2	^{140}Ce$^+$	^{142}Nd$^+$	^{143}Nd$^+$	^{144}Nd$^+$	^{145}Nd$^+$	^{146}Nd$^+$	^{147}Sm$^+$	^{148}Nd$^+$
Interference		^{142}Ce$^+$		^{144}Sm$^+$				^{148}Sm$^+$
S3	^{141}Pr$^+$	^{143}Nd$^+$	^{144}Nd$^+$	^{145}Nd$^+$	^{146}Nd$^+$	^{147}Sm$^+$	^{148}Nd$^+$	^{149}Sm$^+$
Interference			^{144}Sm$^+$				^{148}Sm$^+$	
S4	^{142}Nd$^+$	^{144}Nd$^+$	^{145}Nd$^+$	^{146}Nd$^+$	^{147}Sm$^+$	^{148}Nd$^+$	^{149}Nd$^+$	^{150}Nd$^+$
Interference	^{142}Ce$^+$	^{144}Sm$^+$				^{148}Sm$^+$		^{150}Sm$^+$

Nd isotope ratios were measured by dynamic 4 sequence mode using Isoprobe-T TIMS. This helps to minimize uncertainties due to variations in relative detector efficiencies. Cup configuration of low mass (L2), axial (Ax) and high (H1–H6) masses for measurement of Nd isotopes analyses and isobaric interferences in four sequence measurements are shown. The interfering signals from ^{142}Ce$^+$ and ^{144}Sm$^+$, ^{148}Sm$^+$ and ^{150}Sm$^+$ at masses 142 and 144, 148, and 150 are noted below each sequence. The signals for ^{144}Nd$^+$ in all 4 sequences are corrected for ^{144}Sm$^+$ interference using the ^{147}Sm$^+$ measured in respective sequence and using a ^{144}Sm/^{147}Sm value of 0.204803. The ^{142}Nd$^+$ signal in S1, S2 and S4 are corrected for ^{142}Ce$^+$ interference using the ^{140}Ce$^+$ (S2, L2) and using a ^{142}Ce/^{140}Ce value of 0.125653. The ^{148}Nd$^+$ signal in S2, S3 and S4 were corrected for ^{148}Sm$^+$ interference by using the ^{147}Sm$^+$ signal in the respective sequences, and a ^{148}Sm/^{147}Sm value of 0.749833; and ^{150}Nd$^+$ signal in S4 was corrected for ^{150}Sm$^+$ interference by using the ^{147}Sm$^+$(S4, H3) signal and ^{150}Sm/^{147}Sm value of 0.492328. The mass fractionation correction parameter for each sequence was calculated by using the measured ^{146}Nd/^{144}Nd ratio in each sequence and normalizing it to a standard reference value of 0.7219.

Table 3
Technical comparison of this study with previous methods.

Parameters	This study	Ref. [2]	Ref. [1]
Sample size (mg)	25–30	50–200	200–600
Digestion in	Savillex vial + Parr pressurized vessel	Savillex beaker	Savillex beaker
Acid used	HF + HNO_3	HF + HNO_3	HF + HNO_3
REE separated by	AG®50W-X12 resin	TRU-spec resin	AG®50W-X8 resin
Ce-cut by	Liq–liq extraction	Liq–liq extraction	H_2O_2 added
Na-removed by	AG®50W-X8 resin	AG-50X8 resin	Not done
Nd separated by	Ln-spec resin	Ln-spec resin	2-Methylactic acid
Nd load (ng)	200–250	300–500	Not reported
Filament geometry	Triple	Double	Double
^{142}Nd intensity (A)	$0.8–2.5 \times 10^{-11}$	$4–5 \times 10^{-11}$	$1.6–5 \times 10^{-11}$
Instrument	Isoprobe-T TIMS	Thermo TRITON	Thermo TRITON

Table 4
Nd Isotope data for synthetic and rock standards.

Sample	^{142}Nd[a]	$(^{146}Nd/^{144}Nd)_m$	$^{142}Nd/^{144}Nd$	$^{143}Nd/^{144}Nd$	$^{145}Nd/^{144}Nd$	$^{148}Nd/^{144}Nd$	$^{150}Nd/^{144}Nd$
JNdi-1 #1	4.225	0.721976	1.141862 ± 6	0.512114 ± 6	0.348409 ± 4	0.241582 ± 14	0.236467 ± 20
JNdi-1 #2	4.969	0.722814	1.141859 ± 2	0.512108 ± 2	0.348408 ± 2	0.241598 ± 6	0.236472 ± 8
JNdi-1 #3	5.211	0.723628	1.141864 ± 4	0.512110 ± 2	0.348407 ± 2	0.241598 ± 8	0.236487 ± 10
JNdi-1 #4	5.447	0.722866	1.141859 ± 2	0.512109 ± 2	0.348408 ± 2	0.241606 ± 6	0.236494 ± 8
JNdi-1 #5	5.371	0.723119	1.141863 ± 2	0.512110 ± 2	0.348406 ± 2	0.241616 ± 6	0.236489 ± 8
JNdi-1 #6	5.484	0.722954	1.141853 ± 2	0.512107 ± 2	0.348408 ± 2	0.241593 ± 6	0.236478 ± 8
JNdi-1 #7	5.432	0.723465	1.141850 ± 4	0.512108 ± 4	0.348408 ± 2	0.241600 ± 8	0.236475 ± 12
JNdi-1 #8	5.323	0.723466	1.141858 ± 2	0.512108 ± 2	0.348408 ± 2	0.241594 ± 6	0.236474 ± 8
JNdi-1 #9	5.390	0.723116	1.141848 ± 2	0.512106 ± 2	0.348409 ± 2	0.241606 ± 6	0.236487 ± 8
JNdi-1 #10	4.706	0.723819	1.141850 ± 4	0.512105 ± 4	0.348408 ± 4	0.241608 ± 10	0.236470 ± 12
JNdi-1 #11	5.061	0.723470	1.141850 ± 6	0.512105 ± 4	0.348408 ± 4	0.241583 ± 10	0.236466 ± 14
JNdi-1 #12	4.004	0.722630	1.141858 ± 4	0.512104 ± 2	0.348406 ± 2	0.241582 ± 8	0.236466 ± 10
JNdi-1 #13	3.515	0.723259	1.141849 ± 8	0.512100 ± 6	0.348408 ± 4	0.241590 ± 18	0.236485 ± 22
JNdi-1 #14	4.065	0.723079	1.141864 ± 6	0.512104 ± 4	0.348406 ± 4	0.241581 ± 12	0.236474 ± 14
JNdi-1 #15	4.769	0.723315	1.141872 ± 2	0.512107 ± 2	0.348401 ± 2	0.241588 ± 6	0.236469 ± 8
Mean[b]			1.141857 ± 12	0.512107 ± 13	0.348407 ± 11	0.241595 ± 89	0.236477 ± 78
BCR-2 #1	0.985	0.723938	1.141864 ± 12	0.512629 ± 14	0.348403 ± 14	0.241586 ± 28	0.236486 ± 44
BCR-2 #2	0.927	0.723238	1.141848 ± 16	0.512629 ± 14	0.348402 ± 10	0.241585 ± 30	0.236472 ± 52
BCR-2 #3	1.428	0.721873	1.141851 ± 14	0.512626 ± 10	0.348409 ± 14	0.241598 ± 28	0.236471 ± 40
BCR-2 #4	0.963	0.722902	1.141850 ± 8	0.512623 ± 8	0.348406 ± 8	0.241593 ± 22	0.236476 ± 30
BCR-2 #5	0.780	0.723674	1.141856 ± 18	0.512623 ± 16	0.348395 ± 14	0.241578 ± 46	0.236484 ± 60
BCR-2 #6	2.485	0.722225	1.141851 ± 4	0.512624 ± 4	0.348405 ± 4	0.241574 ± 8	0.236466 ± 14
BCR-2 #7	2.259	0.723408	1.141851 ± 6	0.512627 ± 4	0.348405 ± 4	0.241574 ± 10	0.236478 ± 14
BCR-2 #8	1.405	0.723201	1.141854 ± 12	0.512617 ± 10	0.348401 ± 10	0.241575 ± 28	0.236470 ± 34
BCR-2 #9	1.305	0.723283	1.141857 ± 8	0.512622 ± 8	0.348401 ± 8	0.241567 ± 24	0.236464 ± 28
Mean[b]			1.141854 ± 8	0.512624 ± 15	0.348403 ± 23	0.241581 ± 84	0.236473 ± 65
OL-6 #1[c]	3.437	0.722646	–	0.512629 ± 4	0.348404 ± 4	0.241608 ± 10	0.236460 ± 12
OL-6 #2[d]	4.413	0.722645	1.141878 ± 4	0.512623 ± 2	0.348403 ± 2	0.241590 ± 6	0.236456 ± 8
Mean			–	0.512626	0.348404	0.241599	0.236458
BIR-1 #1	1.960	0.7234316	1.141865 ± 6	0.513080 ± 4	0.348400 ± 4	0.241607 ± 16	0.236458 ± 18
BIR-1 #2	1.385	0.7232148	1.141867 ± 14	0.513078 ± 12	0.348396 ± 10	0.241590 ± 32	0.236467 ± 32
Mean			1.141866	0.513079	0.348398	0.241599	0.236463

The Nd isotope ratios were corrected for mass fractionation using exponential law assuming $^{146}Nd/^{144}Nd = 0.7219$.

[a] The average $^{142}Nd^+$ beam signal strength (in volts as measured on 10^{11} Ω) in sequence S2 (Table 2) is noted for all analyses. The measured value for $(^{146}Nd/^{144}Nd)_m$ in sequence S2 is shown for reference.

[b] Only for JNdi-1 and BCR-2 mean values and the errors are quoted. The error represents (2σ) standard deviation for the measured values, the external precision of our measurements. For BIR-1 and OL-6 the mean values are only indicative.

[c] The OL-6 #1 sample was passed through Ln-spec resin twice which resulted in higher Ce isobaric interference.

[d] The OL-6 #2 sample was passed through Ln-spec resin three times to remove Ce which significantly reduced Ce interference and improved the $^{142}Nd/^{144}Nd$ value.

The quoted errors for fractionation corrected Nd isotopic ratios are 2× sigma mean ($2\sigma_m$) in ppm.

standard JNdi-1 is ~35–50 pA (3.5–5 V) and for rock standards it is ~8–25 pA (0.8–2.5 V) on 10^{11} Ω resistor. A typical measurement consisted of 200 and 400 cycles for rock standards and JNdi-1, respectively. Each cycle consists of 4 sequences and 20 cycles are grouped together to form a block. During analyses the quality of measurement is improved by monitoring and maintaining the signal strength within the specified range for respective samples by adjusting the filament current, focusing unit, and centering the magnet before each measurement block. The measurement matrix for Nd isotopes is shown in Table 2. The background signal strengths or "baselines" are measured for 20 s before each block at ±0.5 amu for all masses for all 4 sequences (Table 2). Comparison of our method with previous studies is tabulated in Table 3.

In this discussion the four sequences in Table 2 as referred to as S1, S2, S3 and S4. In the matrix notation $^{142}Nd(S2, Ax)$ refers to measured signal for ^{142}Nd in sequence 2 in axial cup (Ax). The signal of $^{147}Sm^+$ in all 4 sequences is used for correcting the interference due to respective $^{144}Sm^+$, $^{148}Sm^+$ and $^{150}Sm^+$ isotopes at mass 144, 148 and 150 to correct $^{144}Nd^+$, $^{148}Nd^+$ and $^{150}Nd^+$ signals (see Table 2 for more details). The signal for $^{140}Ce^+$ (Sequence 2) is used for correcting interference of mass $^{142}Ce^+$ at mass 142 on $^{142}Nd^+$ measured in sequences 1, 3 and 4. The mass fractionation correction parameter was calculated by using the measured $^{146}Nd/^{144}Nd$ ratio in each sequence and normalizing it to a standard reference value of 0.7219. In all cases fractionation corrected isotopic ratios were calculated using interference corrected signals strengths.

The dynamic calculation used the matrix array of measured Nd isotopes in 4 sequences to calculate fractionation corrected values for $^{142}Nd/^{144}Nd$, $^{143}Nd/^{144}Nd$ and $^{145}Nd/^{144}Nd$ to reduce the dependency on the uncertainties and temporal fluctuations of faraday cup efficiency. For dynamic calculation, $^{142}Nd^+(S2, Ax)/^{144}Nd^+(S2, H2)$ is corrected for fractionation using $^{146}Nd^+(S4, H2)/^{144}Nd^+(S4, Ax)$; similarly $^{142}Nd^+(S1, H1)/^{144}Nd^+(S1, H3)$ was corrected for fractionation using $^{146}Nd^+(S3, H3)/^{144}Nd^+(S3, H1)$. The square-root of the product of $^{142}Nd/^{144}Nd$ dynamic values represents the reported values. The dynamic calculation for $^{143}Nd/^{144}Nd$ and $^{145}Nd/^{144}Nd$ is more involved compared to that for $^{142}Nd/^{144}Nd$ dynamic values. The dynamic $^{143}Nd/^{144}Nd$ values are calculated as follows: The square-root of the product $^{143}Nd(S1, H2)/^{144}Nd(S1, H3)$ and $^{143}Nd(S2, H1)/^{144}Nd(S2, H2)$ is corrected for fractionation using $^{146}Nd(S3, H3)/^{144}Nd(S3, H1)$. Similarly the values of $^{143}Nd/^{144}Nd$ in sequences 2 and 3 are combined as above and this is corrected for fractionation using $^{146}Nd/^{144}Nd$ in S4 to yield another dynamic value. The square root of the product of dynamic values of $^{143}Nd/^{144}Nd$ represents the reported value. A similar

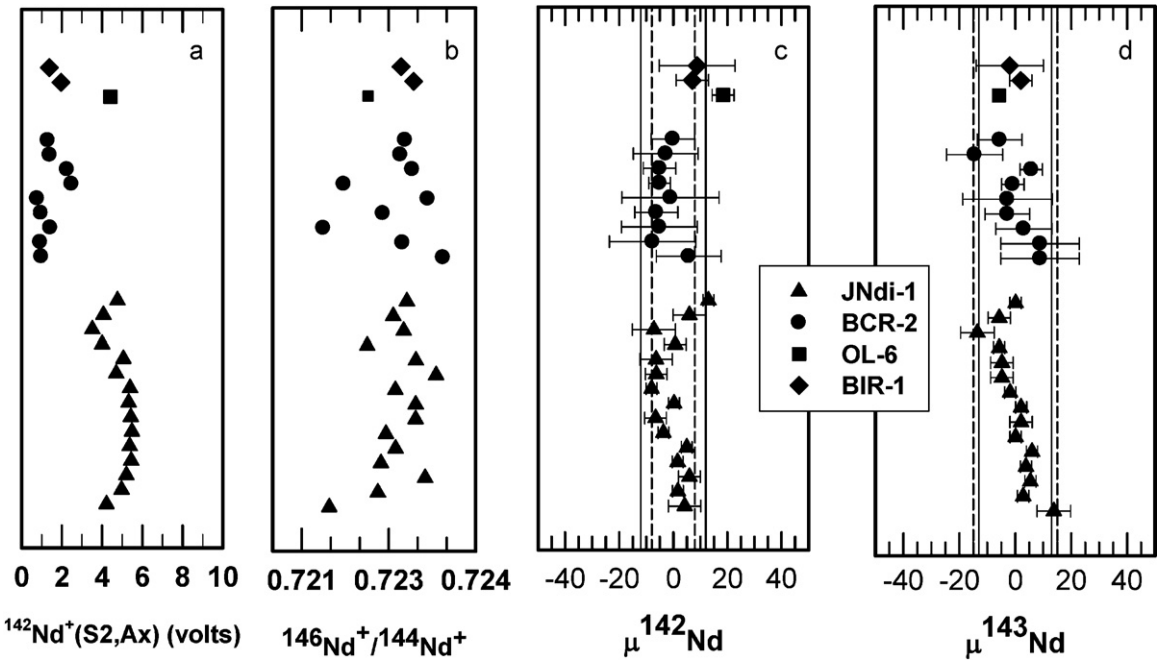

Fig. 3. The Nd data for synthetic standard JNdi-1 and basalt rocks standards, BCR-2, BIR-1 and carbonatite rock sample OL-6 are shown in panels (a, b, c and d) and labelled. The signals Nd isotopes measured in all 4 sequences are corrected for respective interference (Table 2) before further processing of data. The measured ^{142}Nd in sequence 2 (Table 2) in units of volts is shown in panel (a). The measured $^{146}Nd^{+}/^{144}Nd^{+}$ ratio in sequence 2 is shown in panel (b). The deviation of fractionation corrected $^{142}Nd/^{144}Nd$ and $^{143}Nd/^{144}Nd$ from a reference value in units of parts per million (ppm) is plotted as $\mu^{142}Nd$ and $\mu^{143}Nd$ in panels (c) and (d); $\mu^{14i}Nd = [\{(^{14i}Nd/^{144}Nd)_{measured}/(^{14i}Nd/^{144}Nd)_{reference}\} - 1] \times 10^{6}$, and i stands for 2 and 3. The average $^{142}Nd/^{144}Nd$ of 1.141857 for JNdi-1 is the reference value for calculating $\mu^{142}Nd$ values. The average $^{143}Nd/^{144}Nd$ for JNdi-1 is 0.512107; for BCR-2 is 0.512624; BIR-1 is 0.512626; and OL-6 is 0.513079; these values are used for calculating the respective $\mu^{143}Nd$ values. The vertical solid lines and the dashed lines in panels (c) and (d) represent the external precision (twice the standard deviation, 2σ) for JNdi-1 and BCR-2, respectively.

scheme is used for $^{145}Nd/^{144}Nd$. For $^{148}Nd/^{144}Nd$ and $^{150}Nd/^{144}Nd$ the matrix array does not enable calculation of dynamic values and only static values are used.

4. Results and discussion

A chromatographic technique for separation of pure Nd from USGS basalt rock standards, BCR-2 and BIR-1 was established and tested for isotopic results using TIMS. Rock sample of BCR-2 weighing 25–30 mg was used for the calibration of the chromatographic technique using ion exchange column. Rock standard was preferred over synthetic standard for calibration to avoid any potential shift due to matrix effects in the natural sample. The elution schemes for major and minor elements for the two basalt rock standards BCR-2 and BIR-1 are similar. The carbonatite matrix for the OL-6 sample did not cause any significant change in the elution schemes.

The REE species, Ce and Sm which cause significant isobaric interference in Nd isotope measurement were successfully removed to satisfactory levels from the Nd fraction to obtain precise results for $^{142}Nd/^{144}Nd$ and $^{143}Nd/^{144}Nd$ values for rock standards. Initially BCR-2 sample was treated by liquid–liquid extraction (Table 1) on the REE fraction [20] and then eluted using Ln-spec resin with small geometry (0.4 cm internal diameter × 8 cm height) [18] column to achieve complete separation of Ce from Nd. The significant overlap between Ce and Nd fractions because of the broad elution peaks in this small column inhibited complete separation of these two elements. Nd eluted from this column provided excellent results for $^{143}Nd/^{144}Nd$ comparable to published values (Table 4) but not for $^{142}Nd/^{144}Nd$ ratio. These results are not included in further discussion. The column height was increased to 20 cm (Fig. 2) to produce narrow curves of the eluted elements, and thus effectively separate Ce and Sm from Nd for successful measurement of both ^{142}Nd and ^{143}Nd.

The Isoprobe-T TIMS instrument was tested for reliable and reproducible measurement of synthetic Nd standard, JNdi-1; following which Nd separated from rock standards was analyzed for its isotopic composition. The data obtained from JNdi-1 (synthetic standard) and two rock standards BCR-2 (USGS, Columbia River basalt), BIR-1 (USGS, Icelandic basalt), and one carbonatite sample OL-6 (Oldoinyo Lengai, carbonatite lava) are reported in Fig. 3 and Table 4. The measured $^{146}Nd/^{144}Nd$ and dynamic values of $^{142}Nd/^{144}Nd$ are plotted in Fig. 4. The technical parameters and published data from previous studies are compared in Tables 3 and 5, respectively.

The repeated analyses of aliquots of JNdi-1 samples for Nd isotopic composition, using Isoprobe-T TIMS, yielded reliable and reproducible results of high quality over a long period of time. All Nd isotope ratio results from JNdi-1 standards overlap within errors with recently reported results [e.g., 22]. The JNdi-1 average $^{142}Nd/^{144}Nd$ value is 1.141857 ± 12 ppm (2σ, $n = 15$) which overlaps with the average value of 1.141844 ± 9 ppm (2σ, $n = 4$) measured in dynamic mode [22]. The fractionation corrected and dynamic values of $^{142}Nd/^{144}Nd$ and the measured $^{146}Nd/^{144}Nd$ values are not correlated (Fig. 4). The JNdi-1 average value of $^{143}Nd/^{144}Nd$ and $^{145}Nd/^{144}Nd$ are 0.512107 ± 13 ppm (2σ, $n = 15$) and 0.348407 ± 11 ppm (2σ, $n = 15$) which overlap with 0.512126 ± 15 ppm (2σ, $n = 4$) and 0.348414 ± 12 ppm (2σ, $n = 4$), respectively [22]. The $^{148}Nd/^{144}Nd$ and $^{150}Nd/^{144}Nd$ measurements from our JNdi-1 measurements yield less precise values of 0.241595 ± 89 ppm (2σ, $n = 15$) and 0.236477 ± 78 ppm (2σ, $n = 15$) and they overlap with previously reported data of 0.241580 ± 6 ppm (2σ, $n = 4$) and 0.236449 ± 10 ppm (2σ, $n = 4$), respectively [22]. The low abundance of ^{148}Nd and ^{150}Nd compared to ^{142}Nd, ^{143}Nd and ^{144}Nd is one reason for lower precision. The matrix sequence for Nd measurements (Table 2) do not enable calculation of dynamic values for $^{148}N/^{144}Nd$ and $^{150}Nd/^{144}Nd$ and

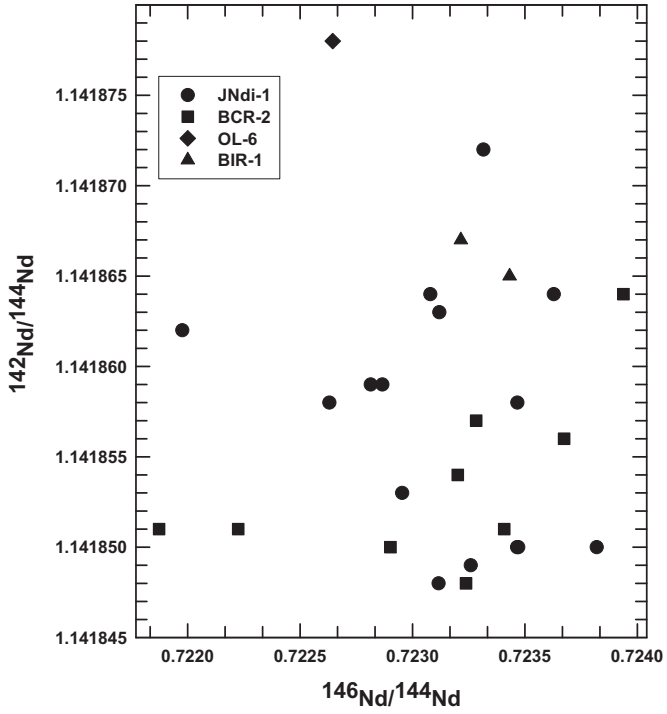

Fig. 4. The measured $^{146}Nd/^{144}Nd$ values (sequence 2) and the fractionation corrected dynamic $^{142}Nd/^{144}Nd$ values (Table 4) are plotted. The data do not show any correlation.

the residual fluctuations in cup efficiencies are not removed. The Isoprobe-T unlike the Triton TIMS [e.g., 1,2,7] is not equipped with virtual matrix rotation of Faraday-cup preamplifiers, and therefore, the fluctuations arising from Faraday cup preamplifiers cannot be eliminated without using dynamic calculation methods.

Multiple aliquots of 30 milligram of BCR-2 was used to test the ability to separate high purity Nd from the rock sample; and determine Nd isotope composition using the same measurement protocols as applied for JNdi-1 standard. The Nd concentration of 28.7 ± 0.2 ppm [23] in BCR-2 made separation of $\sim 250 \times 10^{-12}$ g of Nd possible from a single aliquot of ~30 mg. The BCR-2 Nd yielded high quality results for $^{142}Nd/^{144}Nd$ and $^{143}Nd/^{144}Nd$ and the measured averages for these ratios are 1.141854 ± 8 (ppm, 2σ, $n = 9$)) and 0.512624 ± 15 (ppm, 2σ, $n = 9$), respectively. The $^{143}Nd/^{144}Nd$ values for our BCR-2 Nd measurements overlap with the previously reported results (Table 4). The results for $^{145}Nd/^{144}Nd$ for BCR-2 overlap within errors with the mean value for JNdi-1 Nd data.

The BIR-1 rock standard has an extremely low abundance of Nd, 2.5 ppm [24]. Since the first column (Fig. 1) was calibrated for a maximum of ~30 mg of BCR-2, sufficient Nd for isotopic analyses was achieved by cumulating the REE fraction by processing 4 BIR-1 aliquots (30 mg each). This is a potential disadvantage of our method which resulted in only 2 analyses of BIR-1. The high abundance of Nd, ~128 ppm [19], in OL-6 required processing of only very small amounts of carbonatite sample. However, Nd measurements are inhibited by the very high Ce content of ~565 ppm [19]. Ce removal achieved by single treatment of liquid–liquid extraction followed by double pass elution using the Ln-resin was insufficient, and produced significant Ce interference in ^{142}Nd measurement. After correcting the $^{142}Nd^+$ signal for $^{142}Ce^+$ interference the residual excess in $^{142}Nd/^{144}Nd$ value was more than 30 ppm. This problem was mitigated by a third pass of the sample, OL-6 #2 through the Ln-resin, and the measured $^{142}Nd/^{144}Nd$ ratio overlaps with synthetic standard JNdi-1, and the rock standards, BCR-2 and BIR-1. The $^{143}Nd/^{144}Nd$ ratios measured for both samples of OL-6 #1 and #2 overlap within errors with the previously reported values in literature (Table 5) [19]. As noted earlier Ce interference does not hinder the measurement of $^{143}Nd/^{144}Nd$ ratio which only depends on high quality separation of Sm from Nd. The $^{143}Nd/^{144}Nd$ value for BIR-1 reported in literature over the last 15 years show a spread of nearly 50 ppm (Table 5). The value for the two individual BIR-1 data from this work (Tables 4 and 5) is in the middle of the range of previously published data.

For basalt rock standard BCR-2 an external precision of ±8 ppm (2σ) for $^{142}Nd/^{144}Nd$ values (Tables 4 and 5, Fig. 3c) was obtained. Rock standard BIR-1 with basaltic composition (Tables 4 and 5) has $^{142}Nd/^{144}Nd$ values fall within the envelope of external precision as determined for BCR-2 and JNdi-1. Carbonatite sample, OL-6, falls within a 3σ envelope of the spread of $\mu^{142}Nd$ values in BCR-2. The data reported here is precise for resolving chondritic values which differ from the mean of terrestrial standards by more than 15 ppm. For chondrites the $^{142}Nd/^{144}Nd$ values differ from terrestrial stan-

Table 5
Nd-isotope ratios of synthetic and geological standards measured in this study and literature values.

Sample	n^a	$^{142}Nd/^{144}Nd^a$	$^{143}Nd/^{144}Nd^a$	n[b]	$^{142}Nd/^{144}Nd^b$	$^{143}Nd/^{144}Nd^b$	References
JNdi-1[c]	15	1.141857 ± 12	0.512107 ± 13	112	–	0.512115 ± 7	[14]
				4	1.141844 ± 9	0.512126 ± 15	[22]
BCR-2[e]	9	1.141854 ± 8	0.512625 ± 15	10	–	0.512637 ± 17[d]	[7]
				11	–	0.512634 ± 12	[7]
				1	–	0.512635 ± 4	[17]
				5	–	0.512633 ± 38	[18]
BIR-1[f] #1	1	1.141865 ± 6	0.513080 ± 4	1	–	0.513069 ± 8	[17]
BIR-1#2	1	1.141867 ± 14	0.513078 ± 12	1	–	0.513088 ± 15	[17]
				1	–	0.513094 ± 7	[18]
				1	–	0.513075 ± 7	[18]
OL-6[g] #1	1	–	0.512629 ± 4	1	–	0.51262	[19]
OL-6 #2	1	1.141878 ± 4	0.512623 ± 2				

[a] This study.
[b] Literature value. Absence of measured data for $^{142}/Nd/^{144}Nd$ is denoted by dash (–).
[c] Synthetic Nd standard, available from Geological Survey of Japan [14].
[d] Measured on MC-ICPMS. All other Nd data measured on TIMS. Numbers of replicate analyses are denoted by n. For single measurements errors are reported as twice the standard error of the mean ($2\sigma_m$). For multiple analyses of samples errors are reported as twice the standard deviation (2σ) of the measured population. The number of replicate analyses (n) is noted in parenthesis. For OL-6 #1 the $^{142}Ce^+/^{142}Nd^+$ was $\sim 43 \times 10^{-6}$ making interference correction too large for reliable data. OL-6 #2 sample was eluted 3 times using the Ln-spec resin to reduce the Ce impurity for reliable ^{142}Nd measurement.
[e] Columbia River Flood Basalt.
[f] Icelandic Basalt; and BCR-2 and BIR-1 rock samples available from United States Geological Survey (USGS).
[g] Oldoinyo Lengai, Tanzania (sample loan from Dr. K. Bell [19]).

dards by 10–40 ppm [1]. The lower end of the spectrum, i.e., 10 ppm is represented only by Brudenheim, and 40 ppm end member is represented only by Abee [1]. The majority of samples fall in the range of 15–35 ppm. The precision reported here can successfully resolve the data from average chondritic value even at 200 ng Nd load. It is not possible to distinguish the lowest end member with a 10 ppm difference with terrestrial standards.

5. Conclusions

In conclusion complete dissolution of rock samples as achieved by a two-step digestion procedure, using Savillex vial and Parr acid digestion bomb. Chromatographic column separation techniques were calibrated and tested for isolating major, minor, and trace elements including REE fraction from two types of rock matrix, basalt and carbonatite. The liquid–liquid extraction technique removes bulk of the Ce (~90%) from the REE-fraction. Ln-resin chromatography using 4 mm × 20 cm (internal diameter × length) column provided high purity Nd devoid of Sm and Ce for measurement of Nd isotopes.

From several independent measurements of JNdi-1 high quality values for $^{143}Nd/^{144}Nd = 0.512107 \pm 13$ (ppm 2σ external precision) and $^{142}Nd/^{144}Nd = 1.141857 \pm 12$ (ppm 2σ external precision) were obtained. Several aliquots of USGS rock standard BCR-2 were analyzed for Nd isotope composition and $^{143}Nd/^{144}Nd = 0.512624 \pm 15$ (ppm 2σ), $^{142}Nd/^{144}Nd = 1.141854 \pm 8$ (ppm 2σ) were obtained. The $^{142}Nd/^{144}Nd$ values for geological standards, BCR-2 and BIR-1, from different geological settings fall within the envelope of ± 12 ppm (2σ), the external precision determined for Nd data from JNdi-1 synthetic standard.

Acknowledgements

Dr. Guillaume Caro (CRPG-CNRS) and Dr. D. Papanastassiou (JPL) are thanked for helpful discussions and insights. We thank Dr. Maud Boyet for helpful reviews. Elution Curve calibrations were carried out at Analest ICPAES, University of Toronto. Dr. H. Kamioka's (Geological Survey of Japan) generous support for providing JNdi-1 Nd standard is graciously acknowledged. We are grateful to Dr. K. Bell for providing sample of carbonatite sample (OL-6). Work supported by NSERC, CFI, and University of Toronto. One of the authors (GS) acknowledges the support provided by S. Garde in completing this work.

References

[1] M. Boyet, R.W. Carlson, Science 309 (2005) 576.
[2] G. Caro, B. Bourdan, J.-L. Birck, S. Moorbath, Geochim. Cosmochim. Acta 70 (2006) 164.
[3] J. O'Neil, R.W. Carlson, D. Francis, R.K. Stevenson, Science 321 (2008) 1828.
[4] G. Caro, B. Bourdan, Geochim. Cosmochim. Acta (2010), doi:10.1016/j.gca.2010.02.025.
[5] M. Boyet, R.W. Carlson, M. Horan, Earth Planet. Sci. Lett. 291 (2010) 172.
[6] M. Boyet, J. Blichert-Toft, M. Rosing, M. Storey, P. Télouk, F. Albaréde, Earth Planet. Sci. Lett. 214 (2003) 427.
[7] D. Weis, B. Kieffer, C. Maeschalk, J. Barling, J. De Jong, G.A. Williams, D. Hanano, W. Pretorious, N. Mattielli, J.S. Scoates, A. Goolaerts, R.M. Friedman, J.B. Mahoney, Geochem. Geophys. Geosyst. 7 (2006), doi:10.1029/2006GC001283.
[8] A.D. Brandon, T.J. Lapen, V. Debaille, B.L. Beard, K. Rankenberg, C. Neal, Geochim. Cosmochim. Acta 73 (2009) 6421.
[9] V.C. Bennett, A.D. Brandon, A.P. Nutman, Science 318 (2007) 1907.
[10] G.J. Wasserburg, S.B. Jacobsen, D.J. Depaolo, M.T. McCulloch, T. Wen, Geochim. Cosmochim. Acta 45 (1981) 2311.
[11] M. Boyet, R.W. Carlson, Earth Planet. Sci. Lett. 250 (2006) 254.
[12] M. Sharma, C. Chen, Precamb. Res. 135 (2004) 315.
[13] J. Míková, P. Denková, J. Geosci. 52 (2007) 221.
[14] T. Tanaka, S. Togashi, H. Kamioka, H. Amakawa, H. Kagami, T. Hamamoto, M. Yuhara, Y. Orihashi, S. Yoneda, H. Shimizu, T. Kunimaru, K. Takahashi, T. Yanagi, T. Nakano, H. Fujimaki, R. Shinjo, Y. Asahara, M. Tanimizu, C. Dragusanu, Chem. Geol. 168 (2000) 279.
[15] S. Gao, R.L. Rudnick, H.-L. Yuan, X.-M. Liu, Y.-S. Liu, W.-L. Xu, W.-L. King, J. Ayers, X.-C. Wang, Q.-H. Wang, Nature 432 (2004) 892.
[16] I. Raczek, K.P. Jochum, A.W. Hofmann, Geostand. Newslett. 27 (2003) 173.
[17] C. Pin, D. Briot, C. Bassin, F. Poitrasson, Anal. Chim. Acta 298 (1994) 209.
[18] C. Pin, J. Francisco, S. Zalduegui, Anal. Chim. Acta 339 (1997) 79.
[19] K. Bell, A. Simonetti, J. Petrol. 37 (1996) 1321.
[20] M. Rehkämper, M. Gärtner, S.J.G. Galer, S.L. Goldstein, Chem. Geol. 129 (1996) 201.
[21] W.F. McDonough, S.-S. Sun, Chem. Geol. 120 (1995) 223.
[22] R.W. Carlson, M. Boyet, M. Horan, Science 316 (2007) 1175.
[23] I. Raczek, B. Stoll, A.W. Hofmann, K.P. Jochum, Geostand. Newslett. 25 (2003) 77.
[24] K. Govindaraju, Geostand. Newslett. 19 (1995) 32, special issue.